Space-based InSAR with sub-daily temporal baselines

Evan L. Kramer and Brent M. Minchew

Division of Geological and Planetary Sciences,
California Institute of Technology, Pasadena, CA 91125, USA

Corresponding author: Evan L. Kramer (`elkramer@caltech.edu`)
Brent M. Minchew (`minchew@caltech.edu`)

Preprint statement

This is a non-peer-reviewed preprint submitted to **EarthArXiv**. This manuscript has been submitted to *IEEE Geoscience and Remote Sensing Letters* for peer review. As a non-peer-reviewed preprint, subsequent versions of this manuscript may have differing content.

Space-based InSAR with sub-daily temporal baselines

Evan L. Kramer and Brent M. Minchew

***Abstract*—Interferometric synthetic aperture radar (InSAR) underpins the Surface Deformation and Change observable prioritized by the 2018 decadal survey, yet the temporal sampling of current assets aliases many transient geophysical processes. For single-satellite repeat-pass InSAR, satellite orbits accommodate temporal baselines at integer nodal day intervals down to a single nodal day. Processes that evolve over minutes to a couple days are undersampled by these systems. This work presents a constellation architecture, termed Tunable WIndow for Surface Transients (TWIST), that acquires cross-satellite interferograms at programmable sub-daily temporal baselines by distributing SAR satellites across multiple orbit planes. Orbit phasing as a function of desired temporal baseline is formalized into plane orientation and inter-orbit satellite position conditions that align the satellites' ground tracks in the Earth-fixed frame under J2-perturbed dynamics. Routine science and on-demand operating strategies are evaluated through modeled spatial coverage, average response time, and three-dimensional displacement retrieval feasibility. A four-satellite TWIST InSAR constellation observes 99.8% of global land at sub-daily temporal baselines, achieves an on-demand average response time of 6.7 hr, and offers three-dimensional displacement retrieval for 91.1% of global land. The presented results demonstrate the game-changing observation capabilities of the TWIST InSAR architecture for nine previously identified targeted observables while showing no major technical hurdles in acquisition of the orbit phasing conditions.**

***Index Terms*—SAR, InSAR, Constellation, Orbit design**

I. Introduction and background

New space-based remote sensing architectures are motivated most directly by the questions set forth by science communities. The Decadal Survey for Earth Science and Applications from Space, published by the National Academies of Science, Engineering, and Medicine, prioritizes community-sourced science questions to be addressed over a decade. Its Surface Deformation and Change (SDC) high-priority designated observable groups the cryosphere, ecosystems, hydrology, and solid Earth and geohazards communities, which rely on interferometric synthetic aperture radar (InSAR), among other technologies, for precise deformation measurements. With the next survey anticipated in 2028, several questions from the 2018 survey remain insufficiently addressed, largely for lack of suitable observing systems. In response, a multidisciplinary NASA study team proposed future mission architectures [1], one of which acquires InSAR measurements at sub-daily temporal baselines using a constellation of SAR satellites in multiple orbit planes. This article formalizes the enabling orbit phasing conditions, termed the Tunable WIndow for Surface Transients (TWIST) conditions, investigates a variety of repeat intervals and orbit inclinations, and presents operating strategies and estimated performance in spatial coverage, average response time, and three-dimensional (3D) surface displacement retrieval.

E. Kramer and B. Minchew are with the Division of Geological and Planetary Sciences, California Institute of Technology, Pasadena, CA, 91125 USA e-mail: elkramer@caltech.edu.

TWIST is put forth as a complement to the NASA–ISRO NISAR mission, which is the program-of-record realization of many previously identified targeted observables [2], acknowledging that a single mission cannot address every science community's needs. The 2018 decadal survey needs not met by NISAR fall into two groups [3]: science targets that advance process understanding, such as ice-sheet and glacier mass loss, solid-surface deformation, and the rates at which Earth's surface is reshaped; and hazard monitoring, such as volcanic and interseismic and coseismic fault strain, disaster response, and landslide detection and tracking. Common to all is the need to resolve process temporal evolution through shorter response and revisit times, an emphasis reiterated in a May 2026 review across ten Earth science disciplines that finds six require observations at daily or shorter intervals and nine require revisit more frequent than one week [4].

For single-satellite repeat-pass InSAR, the temporal baseline separating the two acquisitions that form an interferogram is set by the satellite's repeat cycle, which for NISAR is 12 days, and for commercial providers who have already shown capacity to complement NISAR for SDC applications, is seven, three, or one day [5], [6]. In this sense, recovering a time-varying signal is a classical sampling problem such that a process evolving on a timescale comparable to or shorter than the temporal baseline is under-sampled and aliases. Figure 1 shows this trade, plotting an observing system's temporal baseline against the characteristic timescale of the process under observation. A diagonal Nyquist locus divides the plane into a resolved regime, where the baseline is short enough to sample the process faithfully, and an aliased regime, where it is not. Horizontal lines are drawn according to repeat cycles of on-orbit InSAR-capable satellites that adequately sample a process only where the line lies below the Nyquist locus. Processes that occur on timescales up to two days cannot be sufficiently sampled by monolithic observing systems since repeat ground track orbits must occur over an integer number of nodal days. To sample these highly transient processes, a multi-satellite system must be employed that can sample a target location at sub-nodal day intervals.

II. Phasing conditions for a tunable window

Multi-satellite InSAR systems have used coordinated approaches to minimize temporal baselines before. The Sentinel-1 (ESA) and COSMO-SkyMed (ASI) constellations are each

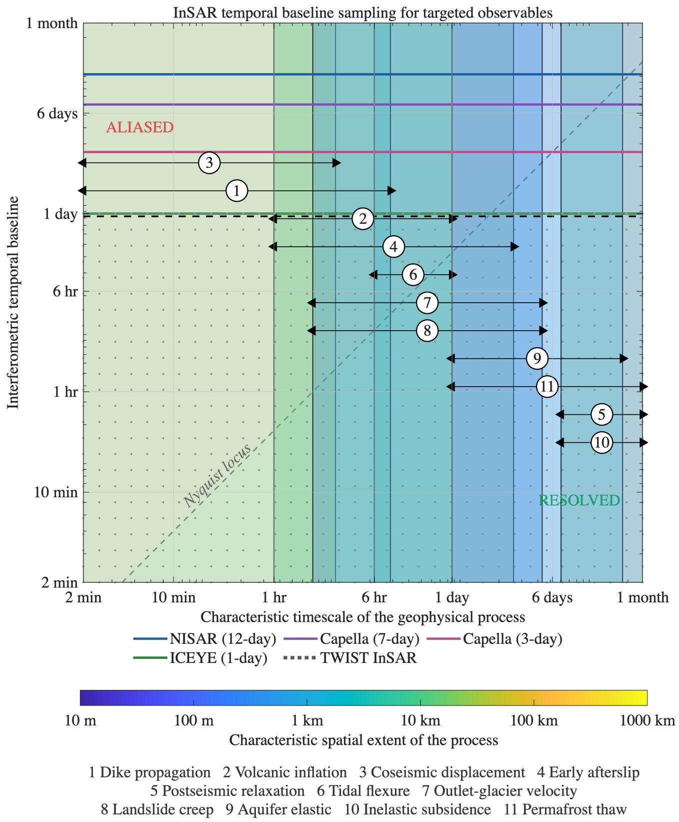

Fig. 1. Top: Geophysical process resolvability for different InSAR observing systems. InSAR temporal baseline is shown on the y-axis and the geophysical process characteristic timescale is shown on the x-axis. A dashed diagonal line indicates the Nyquist sampling locus, demarcating an observing system's ability to resolve a given process. Eleven unique targeted observables from the 2018 SDC report are shown with color shades representative of their characteristic spatial extent.

configured so that observations from different satellites can be combined into an interferogram [7], [8]. Their satellites share a common inertial plane, separated only by argument of latitude. When one passes over a target at time t_0, another in the same plane views it from the same geometry at $t_0 + T_n n_d$, where T_n is the nodal day and n_d an integer. The nodal day is the time for a surface point to complete a full rotation relative to a precessing plane. In an Earth-fixed frame, the satellites trace the same ground track, passing each point at times set by their argument-of-latitude offset. For example, Sentinel-1C and Sentinel-1D each repeat every twelve days, but their 180° phasing yields six-day cross-satellite interferograms, and a temporary 210° phasing between Sentinel-1A and Sentinel-1C reduced this to one day [9]. The first-generation COSMO-SkyMed placed four satellites on a nominal sixteen-day repeat in one plane. A 90° separations among the first, second, and fourth gave four-, eight-, and twelve-day baselines, and a 67.5° offset of the third achieved one-day [10].

Common to all of these configurations is a one-day floor. Sharing a common inertial plane, the satellites can re-observe a target from the same relative geometry only after the Earth completes a full rotation through the plane's nodes. TWIST InSAR unlocks sub-daily baselines by relaxing this common-plane requirement, using two orbit phasing conditions to enable multi-plane cross-satellite InSAR. Contextualizing these conditions requires the definition of a repeat ground track (RGT) orbit, which a satellite traces by completing an integer number of nodal periods n_p in an integer number of nodal days n_d [11]. The ratio n_d/n_p is the similitude parameter τ, related to the satellite's orbital parameters in equation 1.

$$\tau = \frac{n_p}{n_d} \approx \frac{\omega_\oplus - \dot{\Omega}}{n + \dot{\omega}} \tag{1}$$

Satellite mean motion is represented as n, Earth's rotation rate is $\omega_\oplus$, the precession of the satellite's argument of perigee is $\dot{\omega}$, and the precession of the satellite's right ascension of the ascending node (RAAN) is $\dot{\Omega}$. The rate-of-change terms arise from Earth's asymmetric gravitational field, which causes the orbit plane to precess. They can be approximated to first order as shown in equations 2 and 3.

$$\dot{\Omega} = -\frac{3}{2} J_2 \left(\frac{R_E}{p}\right)^2 n \cos(i) \tag{2}$$

$$\dot{\omega} = \frac{3}{4} J_2 \left(\frac{R_E}{p}\right)^2 n \left(5\cos^2(i) - 1\right) \tag{3}$$

Earth's second zonal harmonic coefficient is represented by J_2, Earth's mean equatorial radius by R_E, the semi-latus rectum by $p = a(1 - e^2)$ where a is the semi-major axis and e is the eccentricity, and the inclination by i. Circular orbits ($e = 0$) are assumed in this analysis. To maintain a specific repeat interval, the orbit's semi-major axis and inclination must satisfy equation 1. For near-global coverage, most SAR satellites use sun-synchronous orbits with $i \approx 98°$, leaving the semi-major axis to be found from equation 1 by root-finding [11]. Because equations 2 and 3 retain only the first-order secular $J2$ contribution, this analytic semi-major axis yields a ground track that does not close, so it is refined numerically to minimize the position residual after $J2$-perturbed propagation. For the sun-synchronous orbits considered here, this reduces the closure gap from tens of kilometers to approximately ten centimeters. The two remaining free elements, the argument of latitude u and the RAAN Ω, are leveraged to satisfy the TWIST phasing conditions.

The matched geometry requirement for two InSAR-feasible observations is naturally expressed in the Earth-fixed (ECEF) frame where a reference target location with geodetic coordinates (ϕ, λ, h) is stationary. Given a SAR satellite in a reference RGT orbit, sat_{ref}, its broadside pass of the target occurs when the target lies in the satellite's zero-Doppler plane. The broadside imaging geometry is fully described by the satellite's Earth-fixed position and velocity, $\mathbf{r}^{\text{ECEF}}_{\text{ref,bs}}$ and $\mathbf{v}^{\text{ECEF}}_{\text{ref,bs}}$. Because the target is fixed in this frame, any second satellite that reproduces this same Earth-fixed position and velocity observes the target from an identical broadside pass. The phasing problem reduces to placing a phased satellite, sat_{pha}, at $(\mathbf{r}^{\text{ECEF}}_{\text{bs}}, \mathbf{v}^{\text{ECEF}}_{\text{bs}})$ one temporal baseline, T_{bas}, after sat_{ref} reaches broadside. The temporal baseline itself is a tunable parameter, and given the context provided in section I on the observation gaps present for transient processes, a range of $2\,\text{min} < T_{\text{bas}} < 1\,\text{nodal day}$ is considered, though T_{bas} can be defined as any positive real number.

Transforming this Earth-fixed condition back into the J2000 inertial frame exposes its consequence for the orientation of the phased satellite's orbit plane. Over the interval T_{bas}, the target and $(\mathbf{r}_{\text{bs}}^{\text{ECEF}}, \mathbf{v}_{\text{bs}}^{\text{ECEF}})$ rotate about the true-of-date polar axis through the angle $\xi = \omega_{\oplus} T_{\text{bas}}$. Therefore, the inertial state the phased satellite must occupy at its observation epoch is the reference satellite's broadside state rigidly rotated through ξ about $\hat{\mathbf{z}}$, the Earth's rotation axis at the observation epoch, as shown in equation 4.

$$\begin{aligned}\mathbf{r}_{\text{pha,bs}}^{\text{ECI}} &= R_{\text{PN}}^{\text{T}}\, R_{\hat{\mathbf{z}}}(\xi)\, R_{\text{PN}}\, \mathbf{r}_{\text{ref,bs}}^{\text{ECI}}, \\ \mathbf{v}_{\text{pha,bs}}^{\text{ECI}} &= R_{\text{PN}}^{\text{T}}\, R_{\hat{\mathbf{z}}}(\xi)\, R_{\text{PN}}\, \mathbf{v}_{\text{ref,bs}}^{\text{ECI}}\end{aligned} \tag{4}$$

Since precession and nutation displace the true rotation axis from the J2000 pole, the rigid rotation, $R_{\hat{\mathbf{z}}}$, must be performed about the Earth's rotation axis at the observation epoch rather than the fixed J2000 axis. The precession-nutation matrix, R_{PN}, handles the transformation from the J2000 inertial frame to the true-of-date inertial frame. The reference and phased satellites share the same RGT orbit family designated by τ with equivalent semi-major axes and eccentricities.

While equation 4 completely defines the phased satellite's state relative to the reference satellite's broadside state, the transformation can also be written in terms of orbit elements for a more intuitive geometric representation. The two distinct orbit planes are described relative to each other by a change in RAAN, primarily precipitated by the $R_{\hat{\mathbf{z}}}$ rigid rotation, and inclination, which occurs due to the misalignment between the J2000 inertial z-axis and the true-of-date rotation axis. In the J2000 frame, the phased satellite orbit's angular momentum vector is computed as shown in equation 5.

$$\hat{\mathbf{h}}_{\text{pha}}^{\text{ECI}} = R_{\text{PN}}^{\text{T}}\, R_{\hat{\mathbf{z}}}(\xi)\, R_{\text{PN}}\, \hat{\mathbf{h}}_{\text{ref}}^{\text{ECI}} \tag{5}$$

From the angular momentum vectors, the conditions for RAAN and inclination offsets between the phased and reference satellite orbit plane orientations are computed as shown in equation 6.

$$\begin{aligned}\Delta\Omega &= \text{atan2}\left(\hat{h}_{\text{pha},x}, -\hat{h}_{\text{pha},y}\right) - \text{atan2}\left(\hat{h}_{\text{ref},x}, -\hat{h}_{\text{ref},y}\right) \\ \Delta i &= \arccos\left(\hat{h}_{\text{pha},z}\right) - \arccos\left(\hat{h}_{\text{ref},z}\right)\end{aligned} \tag{6}$$

The final condition for orbit element representation of the Cartesian rigid body rotation is the positioning of the phased satellite in its orbit relative to the reference satellite's position. The argument of latitude is used to represent the angular position of the satellite within its orbit and is defined as $u = \omega + \nu$ where ν is the true anomaly. While ω and ν are individually undefined for the circular orbits considered in this work, the sum of their secular drift rates due to J2 effects is defined: $\dot{u} = \dot{\omega} + \dot{M}$. Note substitution of the mean anomaly for the true anomaly for circular orbits. Under J2-perturbed dynamics, the secular mean anomaly drift rate is given by equation 7.

$$\dot{M} = \frac{3}{2}\frac{J_2 R_{\oplus}^2}{p^2} n \left(1 - \frac{3}{2}\sin i^2\right)\sqrt{1-e^2} \tag{7}$$

Using the secular J2-perturbed rates in equations 3 and 7, the condition for argument of latitude offset is given in equation 8.

$$\begin{aligned}\Delta u &= u_{\text{pha}} - u_{\text{ref}} = -\left(\dot{M} + \dot{\omega}\right) T_{\text{bas}} \\ \Delta u &= -n\left[1 + \frac{3}{2}J_2\left(\frac{R_{\oplus}}{p}\right)^2\left(4\cos^2 i - 1\right)\right] T_{\text{bas}}\ (\text{Mod } 2\pi)\end{aligned} \tag{8}$$

Expression of the argument of latitude offset in the J2000 frame requires compensation for the difference in the position of each orbit's ascending node in the true-of-date frame relative to the J2000 frame as shown in equation 9.

$$\Delta u_{\text{J2000}} = \Delta u_{\text{TOD}} + (\delta_{\text{pha}} - \delta_{\text{ref}}) \tag{9}$$

Equations 6 and 9 constitute the two TWIST InSAR orbit conditions: a plane offset that tracks the Earth's rotation over the temporal baseline and an along-track offset that tracks the satellite's own orbit motion over the same interval. Both depend on the temporal baseline, which itself is a tunable design parameter. Since the reference RGT orbit fixes the orbit elements in equations 6 and 9, definition of T_{bas} fully determines the phased satellite's Ω and u.

III. Modeled performance

To contextualize the TWIST InSAR configuration within SDC priorities, anticipated spatial coverage, average response time, and 3D displacement inversion feasibility are modeled for two operational approaches. In routine science mode (RSM), the SAR look angle is cycled on a fixed schedule from 19° to 47° in two consecutive 14° ranges for a NISAR-like sensor. In on-demand mode (ODM), the look angle and direction are flexibly set to image highly transient events before returning to RSM. Both modes assume electronic antenna steering and run the multi-point cycle in alternating right and left looks directions. All proceeding results were generated for a four satellite constellation with one pair in a 98° inclination and the second in a 56° inclination. Both satellite pairs were phased to produce six hr temporal baselines. Each satellite operates in a RGT orbit with $\tau = 3/43$ resulting in total RSM cycle repeat intervals of twelve days and altitudes of 774 km and 719 km respectively. Modeled performance variability as a function of orbit inclination and RGT orbit family is tabulated in the supplemental material. Figure 2 shows the spatial coverage and average response time for the aforementioned four-satellite TWIST InSAR architecture in RSM and ODM.

In terms of global spatial coverage, all areas with color-coded swaths (99.8%) are observed with a six hour temporal baseline at least once over the twelve day RSM repeat cycle. In terms of average response time after an event occurrence, higher latitudes are generally observed quicker in both RSM and ODM. Band patterns are observed where ground track intersections produce redundant overpasses. Unsurprisingly, the average response time in RSM is an order of magnitude greater compared to ODM demonstrating the strengths of a hybrid operational approach for hazard response.

While the primary motivations for operating satellites with left and right-looking capabilities in unique ground tracks are

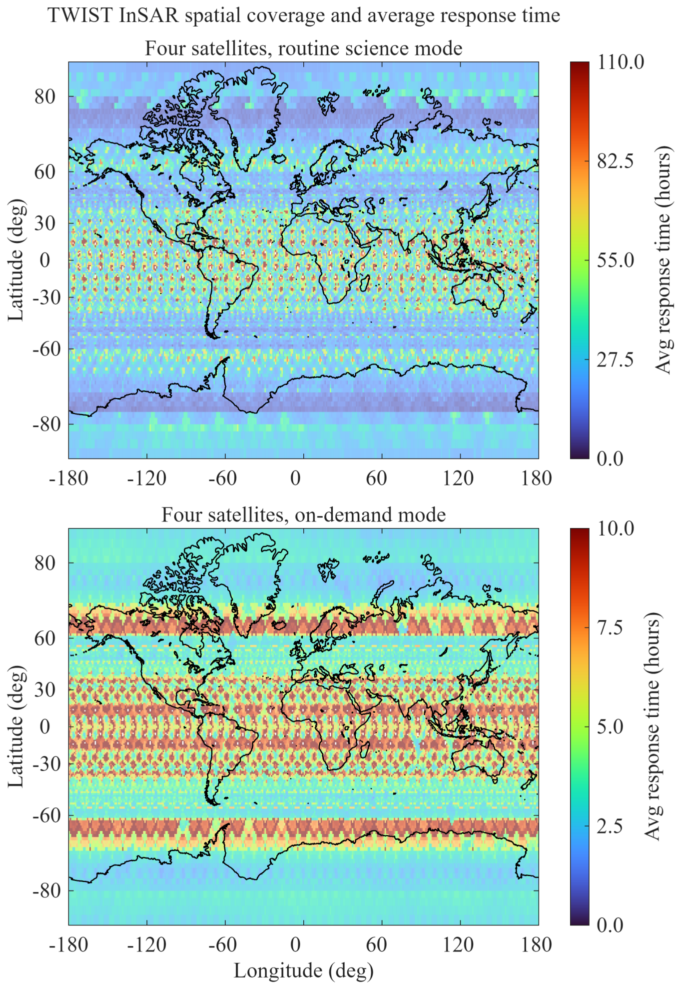

Fig. 2. Spatial coverage and average response time for a four satellite TWIST InSAR constellation in RSM (top) and ODM (bottom). 99.8% of the globe is observable with sub-daily temporal baselines. Swath coverage is color-coded according to the average time until the next available observation after an event.

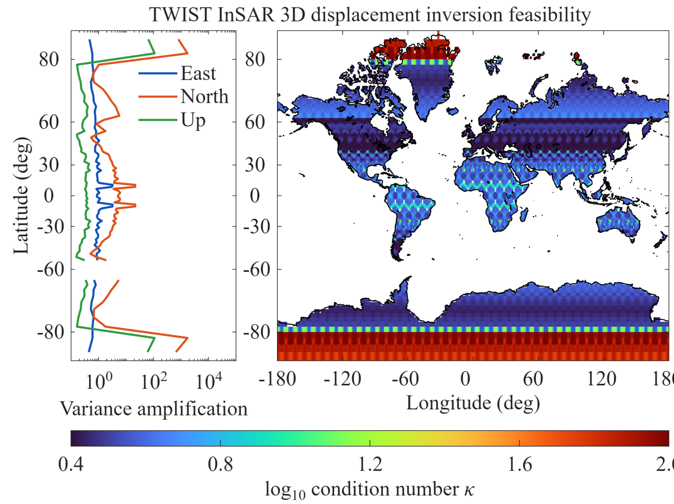

Fig. 3. Stability and error amplification in 3D displacement retrieval for a four satellite TWIST InSAR constellation. Large values for both metrics indicate high inversion sensitivity to noise in observation data. Small periodic gaps in metrics correspond to areas where full 3D displacement retrieval is not feasible without additional data due to an insufficient number of observations with diverse LOS vectors.

increased spatial coverage and decreased average revisit time, the feasibility of 3D displacement inversion also improves. Full 3D displacement retrieval requires a minimum of three independent LOS viewing directions for stable inversion of the design matrix. Figure 3 shows the feasibility of full 3D displacement retrieval by plotting the design matrix condition number, k, on a Mercator map projection and the longitude averaged variance amplification factors (VAF) for the inverted East, North, and Up components as a function of latitude. The smaller the value of k and of the VAF components, the more stable the design matrix inversion. The feasibility of full 3D displacement retrieval covers nearly all land areas (91.1%) and is the most stable around latitudes equal to the orbit inclinations of the four satellite constellation. Unsurprisingly, the North component of the variance amplification factor dominates due to the satellite's along track directions being principally North-South aligned.

IV. Orbit Acquisition and Sensitivities

Since satellites have never operated as TWIST InSAR pairs on-orbit, the practicalities of acquiring such a configuration warrant attention. Satisfying the plane orientation conditions in equation 6 amounts to inserting a satellite into the correct inertial plane at launch where the residual between desired and acquired planes depends on the exact launch time. The top plot in figure 4 quantifies this. A slip of up to half a

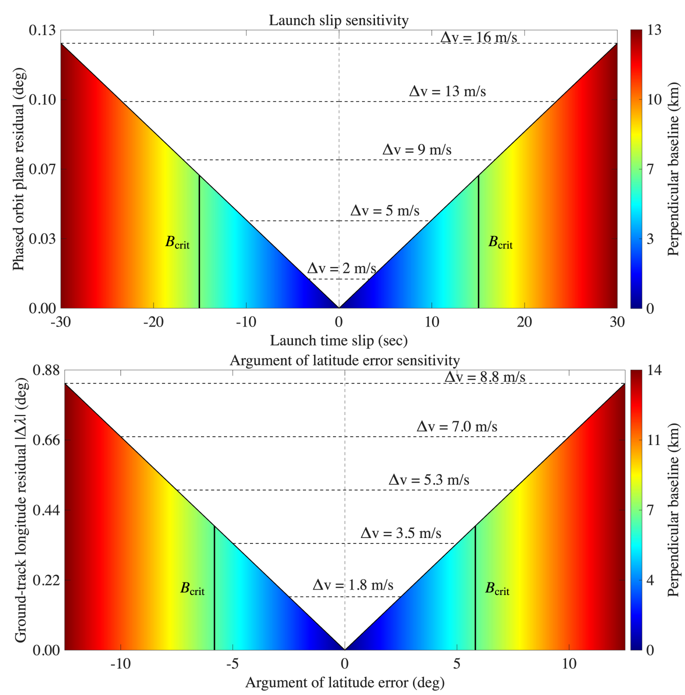

Fig. 4. In both plots, orbit residuals contributing to perpendicular baseline are plotted as colormaps with vertical lines marking the theoretical critical baseline value for X-band systems. Additionally, the out-of-plane and in-plane velocity change magnitudes required to nullify the given orbit residual are shown as dashed horizontal lines. Top: Residual angle between the desired and acquired orbit plane as a function of satellite launch time slip. Bottom: Residual ground track longitude shift between reference and phased satellite as a function of argument of latitude error.

minute produces a plane residual of up to $0.12°$, which maps to a significant perpendicular baseline between the observation pair (colormap). Phase coherence is lost once the perpendicular baseline exceeds the critical baseline (black vertical lines), so coherence is attainable only for launches within a ± 15 s window. The residual can be removed with an out-of-plane velocity change (horizontal dashed lines) that never exceeds 16 m/s across the slips considered, indicating a modest maneuver recovers an off-nominal launch.

Satisfaction of the satellite positioning condition in equation 9 amounts to setting the phased satellite's argument of latitude such that its ground track overlaps the reference satellite's. An error in the phased satellite's argument of latitude results in a longitude shift residual. The bottom plot in figure 4 shows the lateral ground-track longitude residual as a function of argument of latitude error. The shift approaches $0.85°$ for argument of latitude errors of $\pm 12.5°$. A $0.85°$ ground track longitude shift produces significant spatial decorrelation between observation pairs as shown by the color map of perpendicular baseline. The magnitude of the in-plane velocity change is set by the required change in argument of latitude and by the urgency of the desired observation [12]. Assuming a thirty-hour coast orbit, the total velocity magnitude changes to nullify a range of longitude residuals are annotated and are contained within a modest 8.8 m/s. Further discussion on the cost and urgency associated with argument of latitude adjustment can be found in the supplementary material.

V. Conclusion

Drafting of the forthcoming 2028 Decadal Survey for Earth Science and Applications from Space in which recommendations for new observation systems addressing science questions within the surface deformation and change high priority designated observable is imminent. This work expands upon a previous report that presents a candidate observation architecture with InSAR measurements acquired at sub-daily temporal baselines by formally presenting the required orbit phasing conditions. The orbit configuration, here termed Tunable WIndow for Surface Transients (TWIST), has orbit plane orientation and inter-orbit satellite positioning conditions that are a function of the desired temporal baseline. TWIST InSAR performance in terms of spatial coverage, average response time, and 3D displacement inversion feasibility were modeled for different constellation sizes, repeat intervals and orbit inclinations, and operational strategies. Logistics of orbit acquisition and associated sensitivities in relation to InSAR feasibility were investigated. Results show that the TWIST InSAR observation configuration would provide game-changing measurement capabilities for nine targeted observables from the previous decadal survey with outstanding data gaps while not posing major technical hurdles in acquiring the orbit phasing conditions.

References

[1] S. Horst, S. Oveisgharan, E. Tymofyeyeva, A. Khazendar, M. Lavalle, B. Osmanoglu, S. Horner, E. Ford, P. Rosen, and S. Chan, "Constellation concepts for insar observations of earth," *Available at SSRN 6915272*, 2026.

[2] K. Kellogg, P. Hoffman, S. Standley, S. Shaffer, P. Rosen, W. Edelstein, C. Dunn, C. Baker, P. Barela, Y. Shen *et al.*, "Nasa-isro synthetic aperture radar (nisar) mission," in *2020 IEEE aerospace conference*. IEEE, 2020, pp. 1–21.

[3] N. A. of Sciences, Medicine, D. on Engineering, P. Sciences, S. S. Board, C. on the Decadal Survey for Earth Science, and A. from Space, *Thriving on our changing planet: A decadal strategy for Earth observation from space*. National Academies Press, 2019.

[4] C. E. Jones, A. Rosenqvist, B. Rommen, M. Fitrzyk, E. Rignot, B. Scheuchl, Y. Zheng, A. Hooper, M. Simons, T. Kobayashi *et al.*, "Observation and coordination needs for current, near-future, and next generation earth-observing sar systems," *Earth and Space Science*, vol. 13, no. 5, p. e2025EA004868, 2026.

[5] N. Yague-Martinez, V. Cazcarra-Bes, G. Farquharson, C. Stringham, and S. De, "Capella space sar interferometry demonstration: Recent developments and use of mid-inclination orbits," in *IGARSS 2025-2025 IEEE International Geoscience and Remote Sensing Symposium*. IEEE, 2025, pp. 5428–5432.

[6] M. Jo, S. A. Huang, and J. M. Sauber, "Evaluation of the iceye constellation for observing short-term surface displacements induced by volcanic activity," *Remote Sensing Applications: Society and Environment*, p. 102003, 2026.

[7] R. Torres, P. Snoeij, D. Geudtner, D. Bibby, M. Davidson, E. Attema, P. Potin, B. Rommen, N. Floury, M. Brown *et al.*, "Gmes sentinel-1 mission," *Remote sensing of environment*, vol. 120, pp. 9–24, 2012.

[8] F. Covello, F. Battazza, A. Coletta, E. Lopinto, C. Fiorentino, L. Pietranera, G. Valentini, and S. Zoffoli, "Cosmo-skymed an existing opportunity for observing the earth," *Journal of Geodynamics*, vol. 49, no. 3-4, pp. 171–180, 2010.

[9] P. Klenk, K. Schmidt, J. Giez, A. Pulella, M. Nannini, P. Prats-Iraola, and M. Schwerdt, "Independent sar system calibration of sentinel-1 c," *IEEE Journal of Selected Topics in Applied Earth Observations and Remote Sensing*, 2026.

[10] F. Caltagirone, A. Capuzi, A. Coletta, G. F. De Luca, E. Scorzafava, R. Leonardi, S. Rivola, S. Fagioli, G. Angino, M. L'Abbate *et al.*, "The cosmo-skymed dual use earth observation program: Development, qualification, and results of the commissioning of the overall constellation," *IEEE Journal of Selected Topics in Applied Earth Observations and Remote Sensing*, vol. 7, no. 7, pp. 2754–2762, 2014.

[11] D. Mortari, M. P. Wilkins, and C. Bruccoleri, "The flower constellations," *The Journal of the Astronautical Sciences*, vol. 52, no. 1, pp. 107–127, 2004.

[12] R. R. Bate, D. D. Mueller, and J. E. White, *Fundamentals of Astrodynamics*. New York: Dover Publications, 1971.

Evan L. Kramer is the Director's Postdoctoral Fellow in the Seismological Laboratory within the Caltech Geological and Planetary Sciences division. He received a PhD and SM in aeronautics and astronautics from MIT in 2025 and 2022 and a BS in aerospace engineering from the University of Maryland, College Park in 2020. Evan's research interests lie in remote sensing system design, science-aware observation planning, and data processing algorithm development.

Brent M. Minchew is a Professor of Geophysics in the Seismological Laboratory within the Caltech Geological and Planetary Sciences division. He received a PhD in geophysics from Caltech in 2016 and a MS and BS in aerospace engineering from UT Austin in 2010 and 2008. Brent's research interests lie in studying the mechanics of glacier beds, ice rheology, and ice-ocean interactions using satellite radar, mathematical theory, and machine learning to constrain near-term rates of sea level rise.

Supplementary material: Space-based InSAR with sub-daily temporal baselines

Evan L. Kramer and Brent M. Minchew

I. Similitude parameter sweep

In the main text, the spatial coverage, average response time, and 3D surface displacement retrieval feasibility was computed for satellites in three nodal day over forty-three nodal period ($\tau = 3/43$) orbits with mixed inclinations of $98°$ and $56°$. This repeat ground track orbit family has orbit altitudes of approximately 774 km and 719 km respectively. There are a variety of other repeat ground track orbit families and inclination combinations to consider during orbit design with altitudes spanning a larger range of the low Earth orbit regime. To this end, changes in the aforementioned performance measures were quantified for a range of similitude parameters and inclination angles corresponding to a range of low Earth orbit altitudes with repeat intervals from one to three nodal days. Table I presents results for variation in similitude parameter at constant inclination angle.

In the single-pair configuration, increasing the RGT altitude first improves and then degrades performance. Land coverage rises from 61.6% at the minimum altitude to near 93.9% at intermediate altitudes before falling to 73.2% at the maximum altitude. Feasibility of 3D displacement retrieval follows the same rise and fall, peaking in the intermediate range. The average response times exhibit the opposite behavior with both the RSM and ODM times longest at the intermediate altitudes and shortest at the altitude extremes. In terms of the number of TWIST InSAR pairs, performance improves as satellites are added to the constellation at every altitude. Additional pairs raise land coverage and 3D displacement retrieval feasibility and shorten the RSM response time, with the largest step in performance coming from the first to second pair. The 3D displacement retrieval gains are the most pronounced and continue through the third pair, consistent with the added LOS diversity each pair contributes. Land coverage, on the other hand, saturates quickly, approaching or exceeding 90% by the second pair at most altitudes. Of particular note are the single pair 3D-retrieval feasibilities of 52.7% and 59.2% at 665.9 km and 774.2 km which appear to be anomalously high relative to the performance at the three other altitudes. This behavior, and the rise and fall of land coverage percentage as a function of increasing orbit altitude, are explained when the different RGT orbits are considered in terms of their similitude parameters, rather than their altitudes. The mid-altitude cases ($3/44$, $2/29$, $3/43$) repeat over more nodal days and comprise more nodal periods than the single nodal-day repeats at the extremes ($1/15$, $1/14$), producing denser, more geometrically diverse ground-track coverage. In this sense, while increasing RGT orbit altitude does increase the individual projected swath size for a given look angle range, the similitude parameter values must also be considered when selecting a specific RGT orbit that satisfies a given mission's performance objectives.

Table II shows the results for variation in both similitude parameter and inclination angle. Introduction of TWIST InSAR pairs at different inclination angles does not considerably alter performance metrics. In fact, average response time performance slightly degrades. However, figure 1 shows that a closer inspection of the spatial distribution of 3D displacement retrieval feasibility reveals the true added benefit of mixed inclination constellations. Inversion feasibility for the mixed inclination constellation has lower κ, or is more stable, over more land area compared to the $98°$ inclination constellation.

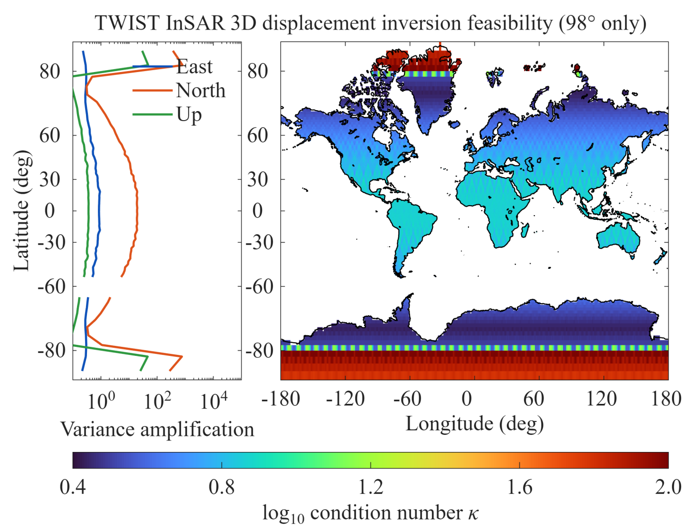

Fig. 1. $98°$ Inclination comparison for the stability and error amplification in 3D displacement retrieval figure in the main text.

II. Maneuver cost and urgency

Acquisition of the TWIST InSAR orbit was described in the main text as minimizing launch time slip and performing in-plane adjustments of the phased satellite's argument of latitude. The operator can tune this adjustment to the maneuver's cost and urgency. The total in-plane velocity change decreases the longer the satellite accumulates lateral longitude shift while in a coast orbit resulting in a less urgent maneuvers costing less. Figure 2 shows how the total velocity change varies with the number of coast orbit revolutions across a range of argument of latitude changes. Urgent maneuvers that demand large argument of latitude changes over few coast

E. Kramer, and B. Minchew are with the Division of Geological and Planetary Sciences, California Institute of Technology, Pasadena, CA, 91125 USA e-mail: elkramer@caltech.edu.

TABLE I
TWIST INSAR PERFORMANCE FOR SIMILITUDE PARAMETERS WITH REPEAT INTERVALS OF ONE TO THREE NODAL DAYS AND 98° INCLINATION.

τ	Inclination (deg)	Altitude (km)	Number pairs	Land coverage (%)	Response time (hr), RSM (ODM)	3D displacement retrieval (%)
1/15	98	561.6	1	61.6	42.6 (6.4)	6.1
1/15	98, 98	561.6, 561.6	2	82.0	32.4 (5.4)	23.6
1/15	98, 98, 98	561.6, 561.6, 561.6	3	87.5	22.6 (4.6)	44.5
3/44	98	665.9	1	91.2	79.9 (14.0)	52.7
3/44	98, 98	665.9, 665.9	2	99.6	44.8 (8.3)	89.3
3/44	98, 98, 98	665.9, 665.9, 665.9	3	99.8	26.4 (5.2)	96.8
2/29	98	719.5	1	89.0	69.2 (11.7)	29.6
2/29	98, 98	719.5, 719.5	2	99.7	39.5 (6.1)	72.4
2/29	98, 98, 98	719.5, 719.5, 719.5	3	99.9	24.1 (3.9)	96.7
3/43	98	774.2	1	93.9	73.6 (12.5)	59.2
3/43	98, 98	774.2, 774.2	2	99.8	39.4 (7.5)	92.4
3/43	98, 98, 98	774.2, 774.2, 774.2	3	99.9	23.1 (4.7)	96.9
1/14	98	886.8	1	73.2	39.1 (5.8)	11.6
1/14	98, 98	886.8, 886.8	2	93.3	28.5 (4.4)	35.1
1/14	98, 98, 98	886.8, 886.8, 886.8	3	97.7	19.0 (3.4)	65.6

TABLE II
TWIST INSAR PERFORMANCE FOR SIMILITUDE PARAMETERS WITH REPEAT INTERVALS OF ONE TO THREE NODAL DAYS AND INCLINATION ANGLES FROM 98°, 56°, AND 45°.

τ	Inclination (deg)	Altitude (km)	Number pairs	Land coverage (%)	Response time (hr), RSM (ODM)	3D displacement retrieval (%)
1/15	98	561.6	1	61.6	42.6 (6.4)	6.1
1/15	98, 56	561.6, 501.7	2	84.5	35.5 (5.5)	20.8
1/15	98, 56, 45	561.6, 501.7, 492.0	3	91.8	28.4 (4.7)	40.5
3/44	98	665.9	1	91.2	79.9 (14.0)	52.7
3/44	98, 56	665.9, 608.3	2	99.3	47.4 (7.9)	85.7
3/44	98, 56, 45	665.9, 608.3, 599.1	3	99.8	31.2 (5.2)	95.7
2/29	98	719.5	1	89.0	69.2 (11.7)	29.6
2/29	98, 56	719.5, 663.1	2	99.5	43.1 (7.2)	73.5
2/29	98, 56, 45	719.5, 663.1, 654.2	3	99.9	28.2 (4.9)	91.8
3/43	98	774.2	1	93.9	73.6 (12.5)	59.2
3/43	98, 56	774.2, 719.0	2	99.8	40.9 (6.7)	91.1
3/43	98, 56, 45	774.2, 719.0, 710.2	3	99.9	26.4 (4.5)	96.8
1/14	98	886.8	1	73.2	39.1 (5.8)	11.6
1/14	98, 56	886.8, 833.9	2	92.7	29.3 (4.6)	40.7
1/14	98, 56, 45	886.8, 833.9, 825.6	3	98.1	21.7 (3.7)	64.4

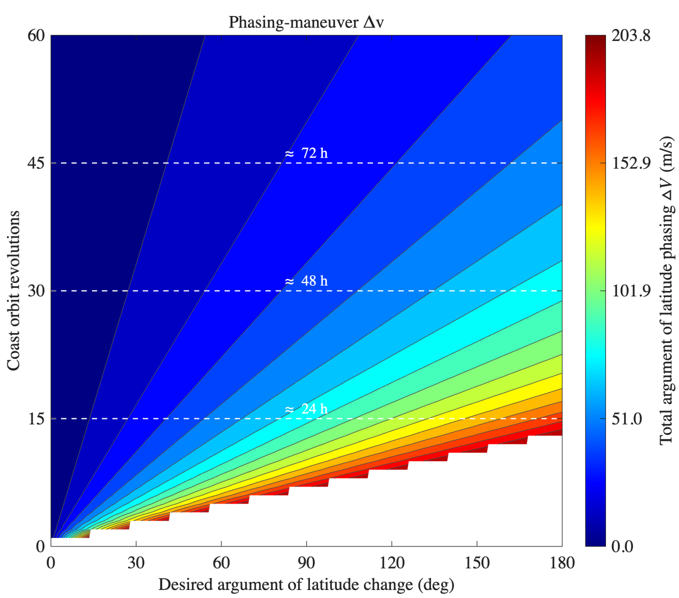

Fig. 2. Total required velocity change magnitude for a range of coast orbit revolutions and argument of latitude changes. The less urgent an argument of latitude change, the less required total velocity change for the maneuvers.

orbit revolutions require substantial total velocity changes upwards of 150 m/s. Less urgent maneuvers require modest total velocity changes of less than 30 m/s even for large argument of latitude changes. As with the plane acquisition maneuver, insertion of the satellite into the desired argument of latitude requires in-plane burns that are conventional in low Earth orbit with the total propellant cost tunable against the acceptable phasing timeline.

Satisfaction of the two TWIST phasing conditions results in a zero spatial baseline repeat-pass InSAR configuration. Intentional deviation from the exact TWIST phasing conditions produces nonzero spatial baselines for repeat-pass InSAR measurements with enhanced topographic height sensitivity. The data shown in the launch slip and argument of latitude sensitivity plots in the main text can be used to design intentional deviations in TWIST phasing conditions to first order for orbit designs that specifically target nonzero spatial baseline architectures. Agile constellation operating strategies that maneuver satellites into and out of TWIST phasing conditions could be investigated to expand the reach of addressable science questions.